Synthesis and Characterization of Coordinatively Unsaturated Alkynyl- and Aryl-Cobalt Complexes with 15 Valence Electrons, $Tp^{iPr2}Co-R$, Bearing the Hydrotris(3,5-diisopropylpyrazolyl)borato Ligand (Tp^{iPr2})

Shin-ichi Yoshimitsu, Shiro Hikichi,† and Munetaka Akita*

Chemical Resources Laboratory, Tokyo Institute of Technology, 4259 Nagatsuta, Midori-ku, Yokohama 226-8503, Japan

Received April 4, 2002

Coordinatively unsaturated 15e alkynyl- ($Tp^{iPr2}Co-C\equiv C-R$) and aryl-cobalt complexes ($Tp^{iPr2}Co$-aryl) bearing the hydrotris(3,5-diisopropylpyrazolyl)borato ligand (Tp^{iPr2}) are prepared by dehydrative condensation of the hydroxo complex $[Tp^{iPr2}Co(\mu\text{-}OH)_2]_2$ with 1-alkyne and arylation of the chloro complex $Tp^{iPr2}Co-Cl$ with Grignard reagents, respectively. Spectroscopic and crystallographic analyses reveal the apparent C_3-symmetrical tetrahedral structures with high-spin electronic configuration ($S = 3/2$), which should result from the property of the Tp^{iPr2} ligand as a tetrahedral enforcer. The $Tp^{iPr2}Co$ and hydrocarbyl fragments are connected dominantly through σ-bonding interaction, and π-interaction including back-donation is not significant as revealed by EHMO calculations. The Co−C bonds are so polarized as to be readily protonated even by moisture to give the corresponding hydrocarbons, but the reactivity toward unsaturated hydrocarbons turns out to be sluggish. $Tp^{iPr2}Co-C\equiv C-COOMe$ is found to catalyze a rare example of specific linear trimerization of methyl propiolate to give (*E*,*E*)-MeOOC(H)C=CH−CH=C(COOMe)−C≡C−COOMe.

Introduction

Coordinatively unsaturated hydrocarbyl species are key intermediates of various transformations mediated by organometallic species, in particular, for the substrate incorporation step.[1] Despite such importance little knowledge concerning their structure and reactivity has been accumulated mainly because of their thermal instability. Most of the previously reported examples of isolable coordinatively unsaturated organometallic species are kinetically stabilized by bulky hydrocarbyl or ancillary ligands such as those bearing trimethylsilyl and mesityl substituents.[2] In previous papers we[3] and other groups[4] reported synthesis and characterization of coordinatively unsaturated 14e and 15e alkyl complexes with κ^3-tripodal ligands [L = hydrotris(pyrazolyl)-borato ($Tp^{R'}$),[5] phenyltris(pyrazolyl)borato, phenyltris-(alkylthiomethyl)borato], LM−R (M = Fe, Co; R = alkyl, benzyl).[6] Despite their coordinatively unsaturated electronic configuration they turned out to be stable with respect to β-hydride elimination, and the stability has been ascribed to the property of the tripodal ligands as a tetrahedral enforcer, which stabilizes the tetrahedral structure with a high-spin electronic configuration, as analyzed by crystallographic and various spectroscopic methods as well as molecular orbital calculations.

The study on the $Tp^{R'}M-R$-type coordinatively unsaturated hydrocarbyl complexes[3] has been extended from the alkyl complexes containing the M−C(sp^3) bond to the alkynyl and aryl complexes containing the M−C(sp) and M−C(sp^2) bond, respectively. For the synthesis of alkyl complexes, it is essential to prevent β-hydride elimination. Although such a problem is not viable in the synthesis of alkynyl and aryl complexes lacking a β-hydrogen atom, oligomerization could be another problem to be solved (Scheme 1).[7] Coupling of the coordinatively unsaturated metal center and the electron-rich π-system may lead to the formation of a

† Present address: Department of Applied Chemistry, School of Engineering, University of Tokyo, Hongo, Bunkyo-ku, Tokyo 113-8656, Japan.

(1) Yamamoto, A. *Organotransition Metal Chemistry*; Wiley-Interscience: New York, 1986. Collman, J. P.; Hegedus, L. S.; Norton, J. R.; Finke, R. G. *Principles and Applications of Organotransition Metal Chemistry*, 2nd ed.; University Science Books: Mill Valley, 1987. Crabtree, R. H. *The Organometallic Chemistry of the Transition Metals*, 3rd ed.; Wiley-Interscience: New York, 2001. Cornils, B.; Herrmann, W. *Applied Homogeneous Catalysis with Organometallic Compounds (2 vols.)*; VCH: Oxford, 1996. Abel, E. W.; Stone, F. G. A.; Wilkinson, G. *Comprehensive Organometallic Chemistry II*; Pergamon: Oxford, 1995.

(2) Examples of Mn, Co, and Fe complexes: Mn: Howard, C. G.; Girolami, G. S.; Wilkinson, G.; Thornton-Pett, M.; Hursthouse, M. B. *J. Chem. Soc., Dalton Trans.* **1983**, 2631. Buttrus, N. H.; Eaborn, C.; Hitchcock, P. B.; Smith, J. D.; Sullivan, A. C. *J. Chem. Soc., Chem. Commun.* **1985**, 1380. C: Morris, R. J.; Gilorami, G. S. *Organometallics* **1989**, *8*, 1478. Wehmschulte, R.; Power, P. P. *Organometallics* **1995**, *14*, 3264. Hursthouse, M. B.; Izod, K. J.; Motevalli, M.; Thornton, P. *Polyhedron* **1996**, *15*, 135. Fe: Chatt, J.; Shaw, B. L. *J. Chem. Soc.* **1961**, 285. Hermes, A. R.; Girolami, G. S. *Organometallics* **1987**, *6*, 763. Müller, H.; Seidel, W.; Görls, H. *J. Organomet. Chem.* **1992**, *445*, 133. Müller, H.; Seidel, W.; Görls, H. *Angew. Chem., Int. Ed. Engl.* **1995**, *34*, 325. Klose, A.; Solari, E.; Floriani, C.; Chiesi-Villa, A.; Rizzoli, C.; Re, N. *J. Am. Chem. Soc.* **1994**, *116*, 9123. Leung, W.-P.; Lee, H. K.; Weng, L.-H.; Luo, B−S.; Zhou, Z.-Y.; Mak, T. W. C. *Organometallics* **1996**, *15*, 1785. Hursthouse, M. B.; Izod, K. J.; Motevalli, M.; Thornton, P. *Polyhedron* **1996**, *15*, 135. Fryzuk, M. D.; Leznoff, D. B.; Ma, E. S. F.; Rettig, S. J.; Young, V. G. Jr. *Organometallics* **1998**, *17*, 2313. Co: Theopold, K. H.; Silvestre, J.; Byrne, E. K.; Richeson, D. S. *Organometallics* **1989**, *8*, 2001. Hay-Motherwell, R. S.; Wilkinson, G.; Hussain, B.; Hursthouse, M. B. *Polyhedron* **1990**, 9, 931. Hursthouse, M. B.; Izod, K. J.; Motevalli, M.; Thornton, P. *Polyhedron* **1996**, *15*, 135. Fryzuk, M. D.; Leznoff, D. B.; Thompson, R. C.; Rettig, S. J. *J. Am. Chem. Soc.* **1998**, *120*, 10126.

10.1021/om020268u CCC: $22.00
Publication on Web 07/31/2002

Scheme 1

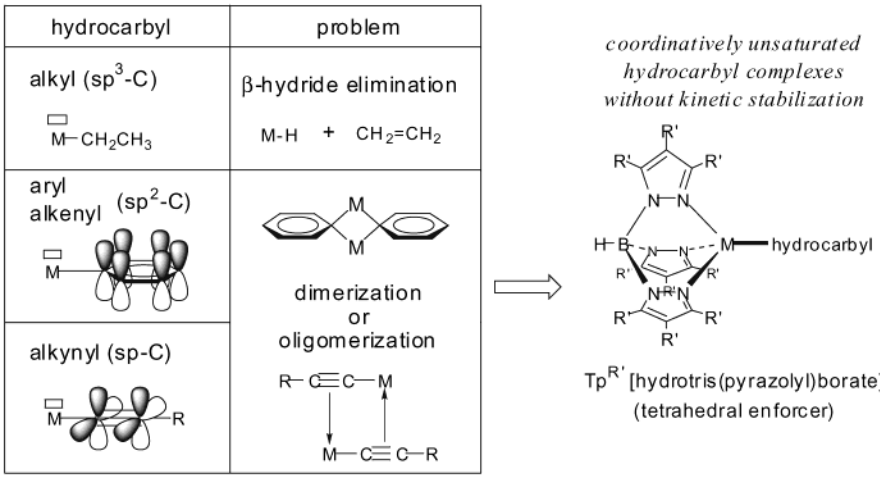

dimeric or oligomeric structure, and many such examples have been reported so far. This problem could also be solved by using the $Tp^{R'}$ ligand. Herein details of the results of the synthetic study of the alkynyl-($Tp^{iPr2}Co-C\equiv C-R$ **1**) and aryl(*p*-tolyl)-cobalt complexes ($Tp^{iPr2}Co-p$-tolyl **2**) will be described.

Results and Discussion

Synthesis and Characterization of Alkynyl Complexes, $Tp^{iPr2}Co-C\equiv C-R$. (i) Synthesis. First attempts to prepare the alkynyl complexes by treatment of the chloro complex, $Tp^{iPr2}Co-Cl$ (**3**), with alkynylating reagents [(1) R−C≡C−Li; (2) R−C≡C−MgBr; (3) R−C≡C−H/Cu(I) cat./amine[8]] were unsuccessful. Reaction (1) afforded $Tp^{iPr2}Li$ via metal exchange, and the other reactions resulted in recovery of **3** or $Tp^{iPr2}Co-X$.

Synthetic study of dioxygen complexes has been a target of our recent research activity,[9,10] and we have developed a new synthetic method for dioxygen complexes (i.e., dehydrative condensation) in addition to the classical method involving O_2-oxidative addition to a low-valent precursor. The dehydrative condensation proceeds via water elimination from the hydroxo complex, $[Tp^{R'}M-OH]_n$ (n = 2, 1), and hydrogen peroxide. Because the terminal hydrogen atom of 1-alkynes is known to be more acidic than other hydrocarbons, 1-alkynes may undergo dehydrative condensation with the dinuclear μ-hydroxo complex bearing the Tp^{iPr2} ligand, $[Tp^{iPr2}Co(\mu\text{-}OH)]_2$, **4**. As we expected, the desired alkynyl complexes **1** were obtained successfully (Scheme 2). We already reported formation of enolatopalladium complexes, $(Tp^{R'})(py)Pd-CHXY$ or $(Tp^{R'})(py)Pd-XCHY$, via dehydrative condensation between the pyridine-coordinated monomeric hydroxo complex, $(Tp^{iPr2})(py)$-

Scheme 2

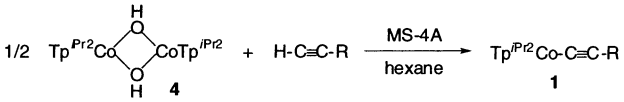

R	amount of 1-alkyne (equiv.) [a]	reaction time (hrs)	yield (%)
COOMe (**1a**)	1.2 (19.1) [b]	2	75
COOEt (**1b**)	1.2	2	76
COMe (**1c**)	1.1	3	62
$SiMe_3$ (**1d**)	2.0 (21.1)	18	60
$SiEt_3$ (**1e**)	2.5	24	70
$SiPh_3$ (**1f**)	1.5	24	0 [c]
H (**1g**)	- [d] (21.7)	1	40 [e]
Ph (**1h**)	1.5 (21.2)	8	48 [e]
t-Bu (**1i**)	2.0 (22.2)	24	56 [e]

[a] Values in parentheses are pK_a values for 1-alkyne observed in H_2O.
[b] pK_a values for H-C≡C-C(=O)-Ph. ref. 13.
[c] $Tp^{iPr2}Co-OSiPh_3$ (**5**) was obtained. See text.
[d] Acetylene gas was bubbled through the reaction mixture.
[e] not isolated in a pure form. See text.

(3) Akita, M.; Shirasawa, N.; Hikichi, S.; Moro-oka, Y. *J. Chem. Soc., Chem. Commun.* **1998**, 973. Shirasawa, N.; Akita, M.; Hikichi, S.; Moro-oka, Y. *J. Chem. Soc., Chem. Commun.* **1999**, 417. Shirasawa, N.; Nguyet, T. T.; Hikichi, S.; Moro-oka, Y. Akita, M. *Organometallics* **2001**, *20*, 3582. See also: Uehara, K.; Hikichi, S.; Akita, M. *Organometallics* **2001**, *20*, 5002.

(4) Kisko, J. L.; Hascall, T.; Parkin, G. *J. Am. Chem. Soc.* **1998**, *110*, 10561. Jewson, J. D.; Liable-Sands, L. M.; Yap, G. P. A.; Rheingold, A. L.; Theopold, K. H. *Organometallics* **1999**, *18*, 300. Schebler, P. J.; Mandimutsira, B. S.; Riordan, C. G.; Liable-Sands, L. M.; Incarvito, C. D.; Rheingold, A. L. *J. Am. Chem. Soc.* **2001**, *123*, 331.

(5) Trofimenko, S. *J. Am. Chem. Soc.* **1966**, *88*, 1842. Trofimenko, S. *Inorg. Synth.* **1970**, *12*, 99. Trofimenko, S. *Chem. Rev.* **1993**, *93*, 943. Trofimenko, S. *Scorpionates−The Coordination Chemistry of Polypyrazolylborate Ligands*; Imperial College Press: London, 1999.

(6) Abbreviations used in this paper: Tp^R, hydrotris(pyrazolyl)borato ligands; Tp^{iPr2}, 3,5-diisopropylpyrazolyl derivative; Tp, nonsubstituted derivative; pz^R, pyrazolyl group in Tp^R. 4-pz-H, the hydrogen atom at the 4-position of the pyrazolyl ring. Compound numbers with ′ (prime) are for nickel derivatives.

(7) Copper complexes can be raised as typical examples. Abel, E. W.; Stone, F. G. A.; Wilkinson, G. *Comprehensive Organometallic Chemistry II*; Pergamon: Oxford, 1995; Vol. 3.

(8) Sonogashira, K.; Tohda, Y.; Hagihara, N. *Tetrahedron Lett.* **1975**, *50*, 4467. Bruce, M. I.; Humphery, M. G.; Matisons, J. G.; Roy, S. K.; Swincer, A. G. *Aust. J. Chem.* **1984**, *37*, 1955.

(9) Akita, M.; Hikichi, S. *Bull. Chem. Soc. Jpn.* **2002**, *75*, in press. Hikichi, S.; Yoshizawa, M.; Sasakura, Y.; Komatsuzaki, H.; Moro-oka, Y.; Akita, M. *Chem.−A Eur. J.* **2001**, *7*, 5011. See also references sited in these papers.

(10) For related dioxygen complexes with Tp and tripodal ligands, see: Reinaud, O. M.; Theopold, K. H. *J. Am. Chem. Soc.* **1994**, *116*, 6979. Reinaud, O. M.; Yap, G. P. A.; Rheingold, A. L.; Theopold, K. H. *Angew. Chem., Int. Ed. Engl.* **1995**, *34*, 2051. Theopold, K. H.; Reinaud, O. M.; Doren, D.; Konecny, R. In *Third World Congress on Oxidation Catalysis*; Grasselli, R. K., Oyama, S. T., Gaffney, A. M., Lyons, J. E., Eds.; Elsevier: Amsterdam, 1997; pp 1081−1088. Thyagarajan, S.; Incarvito, C. D.; Rheingold, A. L.; Theopold, K. H. *Chem. Commun.* **2001**, 2198. Mandimutsira, B. S.; Yamarik, J. L.; Brunold, T. C.; Gu, W.; Cramer, S. P.; Riordan, C. G. *J. Am. Chem. Soc.* **2001**, *123*, 9194. Hu, Z.; George, G. N.; Gorun, S. M. *Inorg. Chem.* **2001**, *40*, 4812. Hu, Z.; Williams, R. D.; Tran, D.; Spiro, T. G.; Gorun, S. M. *J. Am. Chem. Soc.* **2000**, *122*, 3556. Diaconu, D.; Hu, Z.; Gorun, S. M. *J. Am. Chem. Soc.* **2002**, *124*, 1564

Scheme 3

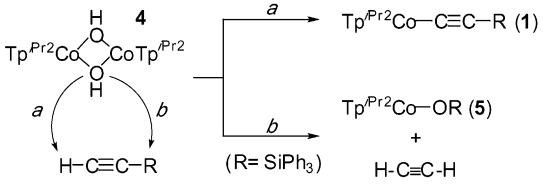

Pd−OH, and active methylene compounds (CH_2XY; X, Y: COR, COOR, CN).[11]

Agitation of a hexane solution of the hydroxo complex **4** and 1-alkyne in the presence of 4 Å molecular sieves afforded the alkynyl complexes **1** as a blue (**1a**−**g**,**i**) or green solid (**1h**) after filtration and crystallization from hexane except for the reaction of triphenylsilylacetylene (see below). It is essential to use hydrocarbon (e.g., hexane, pentane, and toluene) as a reaction solvent.[12] Otherwise the reaction in, for example, THF resulted in incomplete conversion of **4** to give a mixture containing **1** and **4**. In the case of the reaction in a hydrocarbon solvent the eliminated water should be separated from the organic phase due to the extremely low miscibility of water in hydrocarbons, whereas in the case of the reaction in THF the eliminated water remains in the organic phase so as to hydrolyze the product **1** back to **4**.

The efficiency of the condensation depends on the acidity of 1-alkyne. The pK_a values of representative 1-alkynes are shown in the table of Scheme 2.[13] The reaction of acidic substrates bearing a >C═O functional group (**a**−**c**) was almost completed upon mixing, but analytically pure samples of **1g**−**i** derived from the alkyl- or aryl-substituted 1-alkynes could not be obtained due to the slow and incomplete conversion. Complexes **1g**−**i** were characterized by comparison of their spectroscopic data with those of the fully characterized derivatives.

The reaction of triphenylsilylacetylene did not produce the expected alkynyl complex **1f** but the triphenylsiloxo complex, $Tp^{iPr2}Co-OSiPh_3$, **5**, which was characterized by X-ray crystallography (Figure S3).[14] In contrast to the formation of **1**, which involves abstraction of the terminal hydrogen of 1-alkyne (path *a*; Scheme 3), the siloxo complex **5** should be formed via nucleophilic attack of the hydroxo ligand in **4** at the silicon center (path *b*). The silicon atom in triphenylsilylacetylene should be more electrophilic than that in trialkylsilyl derivatives due to the electron-withdrawing nature of the phenyl groups, though the former is more sterically congested than the latter.

We also attempted synthesis of the nickel derivatives, $Tp^{iPr2}Ni-C\equiv C-R$, via a similar procedure. The ester derivative, $Tp^{iPr2}Ni-C\equiv C-COOMe$, **1′**,[6] obtained as pink powders by reaction at 0 °C followed by workup at −30 °C, was identified by its IR data (ν_{BH} 2536, $\nu_{C\equiv C}$ 2099, $\nu_{C=O}$ 1700 cm^{-1}), similar to that of **1a** (see below), and an FD-MS spectrum containing the molecular ion peak (m/z = 606). In the reactions of other 1-alkynes the color change from green to pink or red suggested formation of tetrahedral species, but the mixture further turned to brown or red-brown during workup and no characterizable product could be isolated. In this case, too, the reaction of $Ph_3Si-C\equiv C-H$ afforded the triphenylsiloxo complex, $Tp^{iPr2}Ni-OSiPh_3$, **5′** (characterized by X-ray crystallography; Figure S3),[14] via Si attack (Scheme 3).

Table 1. Spectroscopic Data for Alkynyl Complexes 1

	IR/cm^{-1} [a]			^{1}H NMR/δ_H [f,g]		
complex	ν_{B-H}	$\nu_{C\equiv C}$ ($\Delta\nu$)[b]	ν_R ($\Delta\nu$)[b]	Me	C*H*Me$_2$	4-pz-H
1a	2581	2102 (24)	1697 (22)[c]	3.1, 3.7	11.8	70.0
1b	2574	2094 (24)	1693 (23)[c]	2.9, 3.8	11.8	70.8
1c	2547	2075 (21)	1658 (27)[c]	2.9, 3.8	12.0	70.6
1d	2544	2036 (0)		1.8, 3.9	11.5	68.0
1e	2540	2034 (2)		1.8, 3.9	11.5	68.5
1g	2543	[d]	3287[e]	2.2, 3.8	11.0	68.9
1h	2543	[d]		2.3, 3.8	10.9	68.5
1i	2541	2091 (14)		1.7, 3.8	10.5	67.3

[a] Observed as KBr pellets. [b] Values in parentheses refer to the extent of red-shift of the ν values compared with the corresponding 1-alkynes. [c] $\nu_{C=O}$. [d] Not observed. [e] $\nu_{\equiv C-H}$. [f] Observed as C_6D_6 solutions. [g] Signals for R part: **1a**, 18.6 (3H); **1b**, not obsbd; **1c**, 18.6 (3H); **1d**, 8.9 (9H); **1e**, not observed; **1g**, 12.6 (1H); **1h**, 21.9 (2H), −11.2 (2H), −13.2 (1H); **1i**, 24.4 (9H). [h] The other CH signals could not be located.

(ii) Characterization. The alkynyl complexes **1** are characterized by spectroscopic and crystallographic methods. Selected spectroscopic data are summarized in Table 1. Molecular structures of **1a**,**e** are shown in Figure 1, and selected structural parameters are listed in Table 2.

Formation of the desired structure was first suggested by the changes of IR spectra [(i) disappearance of the ν_{OH} vibration of **4** and $\nu_{\equiv CH}$ vibration of 1-alkyne; (ii) the ν_{BH} absorptions indicating κ^3-coordination;[15] (iii) shift of the $\nu_{C\equiv C}$ and $\nu_{C=O}$ (when appropriate) vibrations to lower energies]. The IR data will be discussed in detail later in combination with the result of the crystallographic structure determination. The simple ^{1}H NMR pattern reveals an apparently C_3-symmetrical structure of **1**. The Tp^{iPr2} signals appear in a similar region irrespective of the alkynyl substituent (R),[16] although one of the two methine signals of the isopropyl groups in the Tp^{iPr2} ligand could not be located presumably due to overlap with other signals or broadening. The monomeric structures are supported by the results of FD-MS data (see Experimental Section). UV spectra featured by the two intense absorptions around 300 and 650 nm are typical for high-spin, tetrahedral $Tp^RCo(II)$ species, as already discussed for the alkyl complexes.[3,4] The high-spin electronic configuration is also supported by the effective magnetic moment (μ_{eff} = 3.4−3.6 μB), suggesting a quartet electronic configuration containing three unpaired electrons (S = 3/2).[17]

(11) Kujime, M.; Hikichi, S.; Akita, M. *Organometallics* **2001**, *20*, 4049.

(12) We also examined synthesis of other $Tp^{R'}$ derivatives such as 3,5-dimethyl and 3-phenyl-5-methyl derivatives. Although dehydrative condensation proceeded, the low solubility of the hydroxo complexes in hydrocarbons resulted in incomplete conversion. Therefore synthesis of alkynyl complexes via dehydrative condensation is applicable only for $[Tp^{R'}M(OH)]_n$ complexes soluble in hydrocarbons.

(13) Kresge, A. J.; Pruszynski, P. *J. Org. Chem.* **1991**, *56*, 4808. Tupitsyn, I. F.; Popov, A. S.; Shibaev, A. Yu. *Zh. Obsh. Khim.* **1992**, *62*, 2757.

(14) For details, see Supporting Information.

(15) Akita, M.; Ohta, K.; Takahashi, Y.; Hikichi, S.; Moro-oka, Y. *Organometallics* **1997**, *16*, 4121.

(16) The Tp^{iPr2} signals (^{1}H NMR) are also comparable to those of the alkyl complexes.[3]

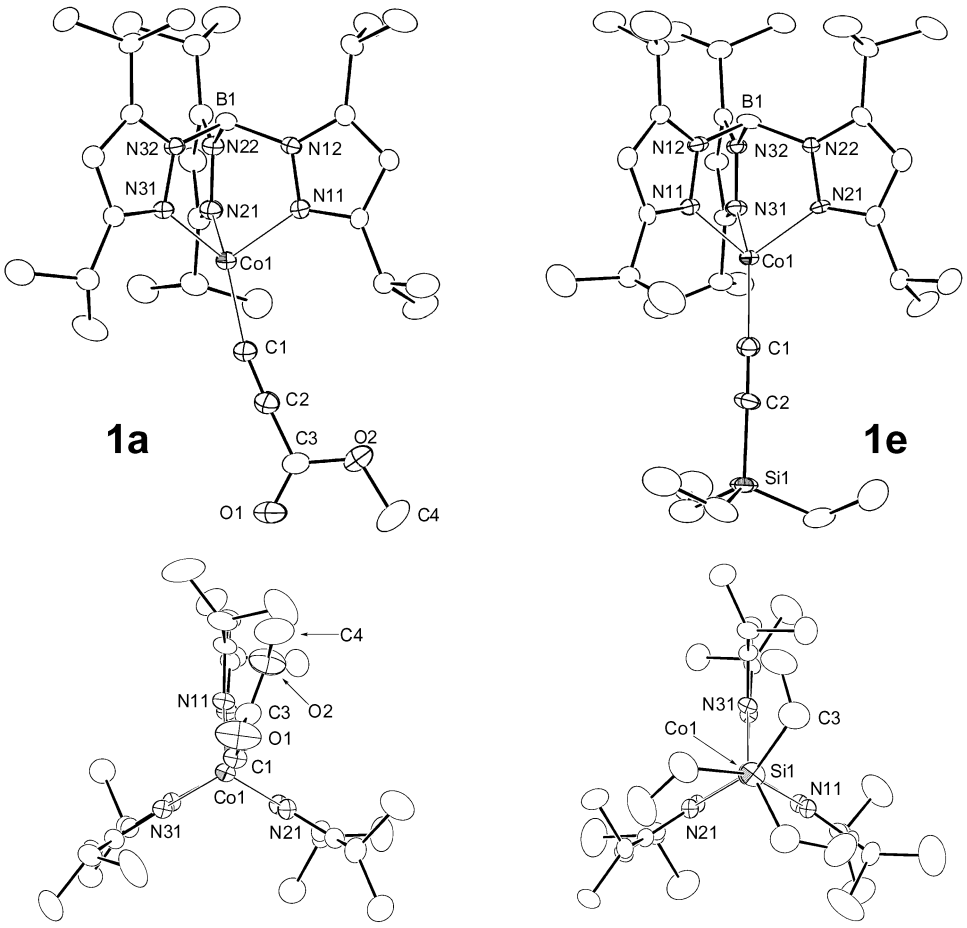

Figure 1. Molecular structures of **1a** and **1e** (one of two independent molecules; A-series) showing 30% thermal ellipsoids.

Table 2. Selected Structural Parameters for Tp^{iPr2}Co−C≡C−R and Tp^{iPr2}Co-*p*-tolyl[a]

complexes	**1a**[b]	**1e**[c] SiEt$_3$		**2**[f]
R	COOMe	molecule 1[d]	molecule 2[e]	
Co−C1	1.968(4)	1.965(6)	1.935(6)	2.011(3)
Co−N11	2.020(3)	2.037(5)	2.034(5)	2.037(3)
Co−N12	2.018(3)	2.010(5)	2.014(3)	2.057(2)
Co−N31	2.043(3)	2.019(5)	1.990(5)	2.060(3)
C1−C2	1.190(6)	1.199(8)	1.233(9)	
C2-X	1.438(6)	1.849(6)	1.804(8)	
X:	C3	Si1	Si2	
Co1−C1−C2	169.0(4)	179.0(6)	178.9(6)	
C1−C2−X	175.1(4)	177.9(8)	174.4(9)	
N11−Co−C1	112.7(1)	123.2(3)	126.5(3)	120.0(1)
N21−Co−C1	121.1(1)	124.4(3)	121.2(2)	124.2(1)
N31−Co−C1	132.9(1)	122.7(2)	121.5(3)	126.3(1)
N11−Co−N21	94.8(1)	91.8(2)	91.8(2)	93.5(1)
N11−Co−N31	93.1(1)	93.2(2)	92.5(2)	90.8(1)
N21−Co−N31	93.5(1)	92.7(2)	94.9(2)	92.97(9)
B···Co−C1	167.7(1)	179.2(2)	176.3(3)	176.1(1)

[a] Bond lengths in Å and bond angles in deg. [b] O1−C3, 1.181(6); O2−C3, 1.330(6); O2−C4, 1.435(8) Å; C1−C2−C3, 175.1(4); O1−C3−O2, 122.0(5); O1−C3−C2, 126.9(5); O2−C3−C2, 111.0(4)°. [c] Si−C(Et), 1.86−1.89(1) Å; C(Et)−Si−C(Et), 106.0−111.7(7)°. [d] A-series. [e] B-series. [f] C1−C2, 1.428(5); C1−C6, 1.380(5); C2−C3, 1.384(5); C3−C4, 1.415(5); C4−C5, 1.398(6); C4−C7, 1.501(6); C5−C6, 1.365(5) Å; C−C−C(tolyl), 111.2−126.3(3)°.

These spectroscopic features are consistent with a C_3-symmetrical tetrahedral core structure, which has been confirmed by X-ray crystallography for the COOMe (**1a**) and SiEt$_3$ derivatives (**1e**) (Figure 1 and Table 2). A unit cell of **1e** contains two independent molecules with essentially the same geometry. Bond lengths associated with the Tp^{iPr2}Co−C≡C parts of **1a**,**e** are very similar. The Co−C1 distances in the range 1.935−1.968 Å (average 1.956 Å) are substantially longer than those of the nine alkynylcobalt complexes [1.857−1.948 Å (average 1.887 Å)], which are included in the CSDS database.[18] Because all nine complexes are coordinatively saturated 18e species, the difference in the Co−C≡ lengths should be ascribed to that of the electronic structure (see below). The C≡C lengths of ca. 1.2 Å are comparable to those of alkynes,[19] but it has been known that the C≡C length is not so sensitive to the electronic effect of the substituents. As for the orientation of the alkynyl ligand, the SiEt$_3$ complex **1e** adopts C_3-symmetrical tetrahedral structures, and orientation of the

(17) The effective magnetic moments below the spin-only value (3.8 μB) should be attributed to the fact that diamagnetic corrections were not applied, as pointed out by one of the reviewers.

(18) (a) Basallote, M. G.; Hughes, D. L.; Jimenz-Tenorio, Leigh, G. J.; Vizcaino, M. C.; Jimenz, P. V. *J. Chem. Soc., Dalton. Trans.* **1993**, 1841. (b) Habadie, N.; Dartiguenave, M.; Britten, J. F.; Beauchamp, A. L. *Organometallics* **1989**, *8*, 2564. (c) Kergoat, R.; L. C. Gomes de Lima, Jegat, C.; Berre, N. L.; Kubicki, M. M.; Guerchais, J. E.; Haridon, P. L. *J. Organomet. Chem.* **1990**, *389*, 71. (d) Klein, H. F.; Beck, H.; Hammerschmitt, B.; Koch, U.; Koppert, S.; Cordier, G. *Z. Naturforsch. Teil B* **1991**, *46*, 147. (e) Giese, B.; Zehnder, M.; Neuburger, M.; Trach, F. *J. Organomet. Chem.* **1991**, *412*, 415. (f) Bianchini, C.; Peruzzini, M.; Vacca, A.; Zanobini, F. *Organometallics* **1991**, *10*, 3697. (g) Stringer, G.; Taylor, N. J. Marder, T. B. *Acta Crystallogr., Sect. C* **1996**, *52*, 80. (h) Werner, H.; Xiaolan, L.; Peters, K.; von Schnering, H. G. *Chem. Ber.* **1997**, *130*, 565. (i) Klein, H. F.; Xiaoyan, L.; Sun, H.; Lemke, A. M.; Florke, U.; Haupt, H. J. *Inorg. Chim. Acta* **2000**, *298*, 70.

(19) Smith, M. B.; March, J. *Advanced Organic Chemistry*, 5th ed.; Wiley-Interscience: New York, 2001.

Scheme 4

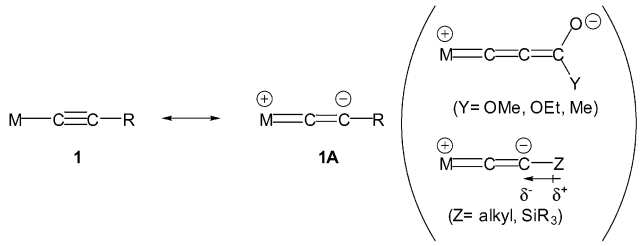

$SiEt_3$ substituent with respect to the $Tp^{iPr2}Co$ moiety is between an eclipsed and staggered conformation, being closer to the former one. The dihedral angles between the N11−Co1−C1 and C2−Si1−C3 planes are 34.2° (molecule 1) and 23.1° (molecule 2).

In contrast to the highly symmetrical structure of **1e**, the structure of the COOMe derivative **1a** is distorted from a C_3-symmetrical one, as is evident from the ORTEP views. The C1−C2 linkage is tilted toward one of the three pyrazolyl rings, as is evident from the B1···Co−C1 angle [167.7(1)°; cf. **1e**: 179.2(2)°, 176.3(3)°]. In addition, the ester plane is arranged closer to a coplanar conformation with respect to one of the three pyrazolyl rings of the Tp^{iPr2} ligand (N11,12−C11−13), and the dihedral angle between the N11−Co1−C1 and C2−C3−O2 planes is 19.8°. Because (1) the more bulky methoxy group is directed toward the bulky pyrazolyl ring and (2) no nonbonded interaction shorter than 2.5 Å is found, the distortion should result from an electronic interaction between the $Tp^{iPr2}Co$ and C≡C−COOMe fragments rather than a steric repulsion and crystal-packing effects, as analyzed by EHMO calculations (see below). No significant difference is observed for the interatomic distances associated with the ester π-system [C2−C3 1.438(6), O1−C3 1.181(6), O2−C3 1.330(6) Å; cf. normal values: ≡C−C═ 1.43, >C═O 1.21, ═C−O 1.34 Å].[19] This situation is in sharp contrast to the coordinatively saturated alkynylcobalt complexes mentioned above [cf. for example, $[(Et_2PCH_2CH_2PEt_2)_2$-(H)Co−COOEt]$^+$ (**6**): Co−C 1.91(1), C≡C 1.19 (2), ≡C−C═ 1.39(2), >C═O 1.18(2) Å],[18a] where back-donation from the cobalt atom to the alkynyl ligand (Scheme 4)[21] occurs, as is evident from the shortened Co−C≡ and ≡C−C═ bonds. In particular, the shortened Co−C≡ distance of **6** compared to those of **1a**,**e** is clear evidence for multiple-bonding interaction (**1A**), i.e., back-donation.

Additional information on the electronic structure of the M−C≡C moiety can be obtained from the IR data. The $\nu_{C\equiv C}$ and $\nu_{C=O}$ vibrations of the alkynyl complexes **1** are shifted to lower energies, as mentioned above, and the extent of the shift is shown in parentheses in Table 1. Substantial shift to lower energies (>20 cm^{-1}) is observed for those containing a >C═O functional group **1a**−**c**, whereas no significant shift is observed for the silyl derivatives **1d**,**e**. The phenyl derivative **1i** is between these two situations. When the IR data are compared with that of **6** [$\nu_{C\equiv C}$ 2076 ($\Delta\nu$ 42); $\nu_{C=O}$ 1658 ($\Delta\nu$ 61) cm^{-1}],[18a] the extent of the lower energy shift of **1a**−**c** is almost half of that of **6**, suggesting that contribution of the back-donation in **1a**−**c** is not as significant as that in **6**. The difference could be attributed to the different electronic configuration of the alkynyl complexes. Thus the $Tp^{iPr2}Co$ complexes **1a**−**c** are highly electron-deficient species with 15 valence electrons, where back-donation does not occur effectively, in contrast to the electron-rich coordinatively saturated 18e species **6**. In conclusion, back-donation is not significant for the electron-deficient $Tp^{iPr2}Co$−C≡C−R species; back-donation contributes to a small extent in the case of alkynyl complexes containing an electron-withdrawing >C═O group (**1a**−**c**), while such contribution is virtually negligible for those containing silyl and alkyl substituents (**1d**−**i**) due to the electron donation from the substituent, which destabilizes the zwitterionic cumulenic resonance structure **1A** (Scheme 4). This conclusion is also supported by the EHMO calculations described below. The back-donation is too weak to freeze free rotation of the Co−C≡ bond to show the apparent C_3-symmetrical ^{1}H NMR features.

(iii) EHMO Calculations. The above-mentioned spectroscopic and structural characterization of the alkynylcobalt complexes **1** reveals some intriguing structural aspects such as (1) stability of the electron-deficient species with 15e configuration, (2) the bending of the Co−C≡C linkage and the coplanar arrangement in **1a**, and (3) dependence of the extent of back-donation on the alkynyl substituent. To consider these problems, EHMO calculations were performed for TpCo−C≡C−$SiMe_3$, **A**, and TpCo−C≡C−COOMe, **B**.[6] An ideal C_{3v}-symmetrical structure was assumed for the TpCo fragment, and the C≡C−$SiMe_3$ and C≡C−COOMe fragments were arranged in the idealized eclipsed and coplanar conformation, respectively, taking into account the results of X-ray crystallography.

Molecular orbitals of the alkynylcobalt complexes **A** and **B** resulting from the interactions of those of the TpCo (**C**) and C≡C−R fragments (**D**, **E**) are shown in Figure 2, where the two fragments are arranged in a linear fashion. The most significant difference in the C≡C−R orbitals (**D**, **E**) is the π^* orbital of the C≡C moiety. In the C≡C−COOMe fragment (**E**) π-conjugation of one of the two C≡C π^* orbitals with the p orbital of the adjacent sp^2-hybridized ester carbon atom causes stabilization of **E**17 (∼−8 eV), while the other three C≡C π^* orbitals (**E**18 and **D**18,19) remain in almost the same higher energy region (>−6 eV). The HOMOs of the C≡C−R fragments (**D**17, **E**16) corresponding to the lone pair electrons are of essentially the same energy level and interact with **C**43 of σ-symmetry to form molecular orbitals for the σ-bonding interaction (**A**47,60, **B**56,60). The rather large energy difference between the orbitals (**C**43 − **D**17/**E**16) renders the M−C σ bond less covalent, as previously revealed for the alkyl complexes by us.[3] As for the π-interaction, orbital **E**17 is low in energy enough to interact with **C**45 (to form **B**59,62), while **D**18,19 and **E**19 of higher energies are left virtually unaffected.

High-spin electronic configuration with $S = 3/2$ result from the large (**A**61,62 − **A**63,64; **B**61 − **B**62) and small energy separations (**A**60 − **A**61,62; **B**59,60 − **B**61);[22] that is, the orbitals up to **A**59 and **B**58 are occupied by

(20) (a) Owsten, P. G.; Rowe, J. M. *J. Chem. Soc.* **1963**, 3411. (b) Ellison, J. J.; Power, P. P. *J. Organomet. Chem.* **1996**, *526*, 263−267. (c) Radonovich, L. J.; Klabunde, K. J.; Berens, C. B.; McCollor, D. P.; Anderson, B. B. *Inorg. Chem.* **1980**, *19*, 1221.

(21) Bruce, M. I. *Chem. Rev.* **1998**, *98*, 2797. See also references therein.

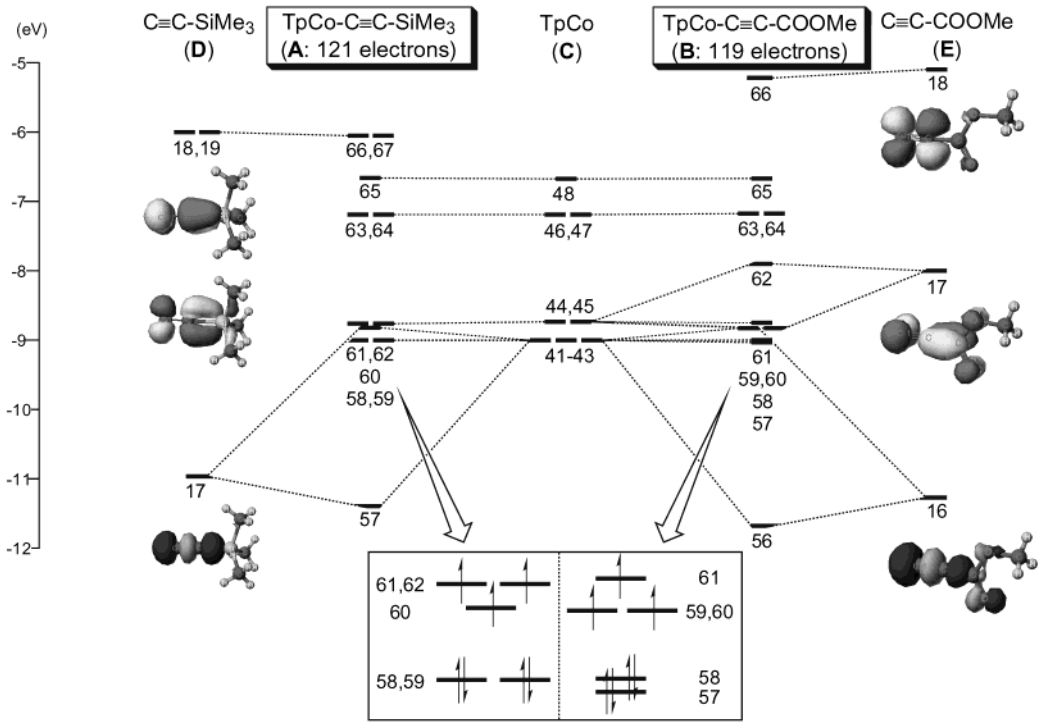

Figure 2. Orbital interactions between the TpCo and C≡C−R fragments.

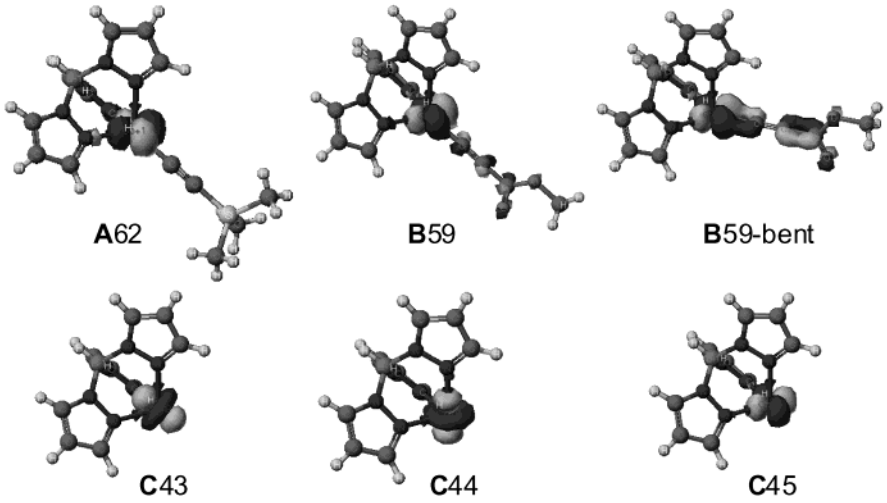

Figure 3. Molecular orbitals of the alkynyl complexes and frontier orbitals of the TpCo fragment.

electron pairs and the orbitals **A**60−62 and **B**59−61 are occupied by unpaired electrons. Such electronic configurations are supported by the result of measurements of magnetic susceptibility.

Thus all frontier orbitals (**A**58−62, **B**57−61) are singly or fully occupied and the lack of a vacant frontier orbital should be the origin of the stability of the electron-deficient 15e species, and essentially the same bonding scheme was already noted for the alkyl complexes.[3,4]

The singly occupied orbital **B**59 (Figure 3) corresponds to π-back-donation from the cobalt center to the C≡C−COOMe ligand. The stabilization obtained by the interaction, however, is not so large that back-donation is not significant, as is consistent with the results of the spectroscopic and crystallographic analyses mentioned above. It is notable for the $SiMe_3$ derivative that the alkynyl fragment virtually does not contribute to **A**62 (Figure 3), indicating the negligible back-donation.

The bending of the Co−C≡C linkage is also explained in terms of the back-donation. Orbital **C**45, which is the metal-based orbital responsible for the back-donation, is shown in Figure 3. As is evident from the shape of the orbital, bending of the Co−C≡ linkage causes effective overlap (**B**59-bent) of the metal-based orbital **C**45 and the π^* orbital of the C≡C−COOMe fragment (**E**17), but, at the same time, the σ-bonding interaction (**C**43 + **E**16) becomes less effective. The arrangement of the C≡C−COOMe ligand should be determined by balance of these two interactions.[23] Judging from the result of the X-ray crystallography the former π-interaction plays a more important role in determining the arrangement. The increased back-donation should also

(22) Shriver, D. F.; Atkins, P. W. *Inorganic Chemistry*, 3rd ed.; Oxford University Press: Oxford, 1999.

cause the coplanar arrangement of the ester plane, as can be seen from the arrangement of **B**59-bent (Figure 3).

Synthesis and Characterization of *p*-Tolyl Complex $Tp^{iPr2}Co-C_6H_4$-*p*-Me, 2. Reaction of the chloro complex **3** with *p*-tolyl Grignard reagent gave the *p*-tolyl complex **2** as moisture-sensitive blue crystals (Scheme 5).[24] An IR spectrum containing the B-H and C(sp^2)-H vibrations [2538, 3043 (KBr pellet); 2543, 3027 cm^{-1} (ether solution)] reveals the presence of a κ^3-Tp^{iPr2} ligand[15] and an aryl group.[25] The ^1H NMR signals for the Tp^{iPr2} moiety are comparable to those of the alkynyl complexes **1**, and the *p*-tolyl signals can also be assigned [δ_H −2.3, 5.4 (9H × 2, CH*Me*$_2$), 14.8 (3H, C*H*Me$_2$; the other CH signal could not be located), 60.3 (3H, 4-pz), −16.3 (2H, tol), 72.0 (2H, tol), 44.2 (3H, *p*-Me)]. Attempted synthesis of the nickel derivative, Tp^{iPr2}Ni-*p*-tolyl, resulted in the formation of an unidentified brown product, although, in this case, too, the color change to pink or red was observed.

Scheme 5

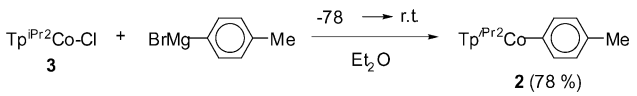

The molecular structure of **2** was determined by X-ray crystallography, and an ORTEP view and selected structural parameters are shown in Figure 4 and Table 2, respectively. The core structure is of virtual C_3-symmetry and the Co−C distance is slightly longer than that in the alkynyl complexes **1**, and the difference (ca. 0.05 Å) is comparable to half of the difference of the C(sp^2)−C(sp^2) (1.48 Å) and C(sp)−C(sp) single bond length (1.38 Å).[19] The aromatic ring is arranged perpendicular to the axial pyrazolyl ring plane, and the orientation could result from release of steric repulsion between the two rings as well as very weak back-donation from **C**44 (Figure 3; see also **M**58 in Figure 5), which is degenerated with **C**45. The *p*-tolyl complex **2** is a member of a rare class of Co(II)−aryl complexes, and, to our knowledge, only three examples of simple nonchelate Co(II)−aryl complexes were reported: $(Et_3P)_2$-Co(mesityl)$_2$ [15e, 1.961(12) Å],[20a] [(μ-Br)(THF)Co−C_6H_3-(*o*,*o*′-mesityl)$_2$] [15e, 2.053(8) Å],[20b] [(η^6-toluene)Co-(C_6F_5)$_2$] [17e, 1.931(5) Å][20c] (electron count and the Co−C length are shown in brackets). It should be noted that all these examples including **2** are electron-deficient species with 15 or 17 valence electrons and that the Co−C length of **2** is comparable to those of the previous examples.

Reactivity of the Alkynyl and *p*-Tolyl Complexes. The hydrocarbyl complexes obtained by the present study were subjected to reactions with various substrates (Scheme 6).

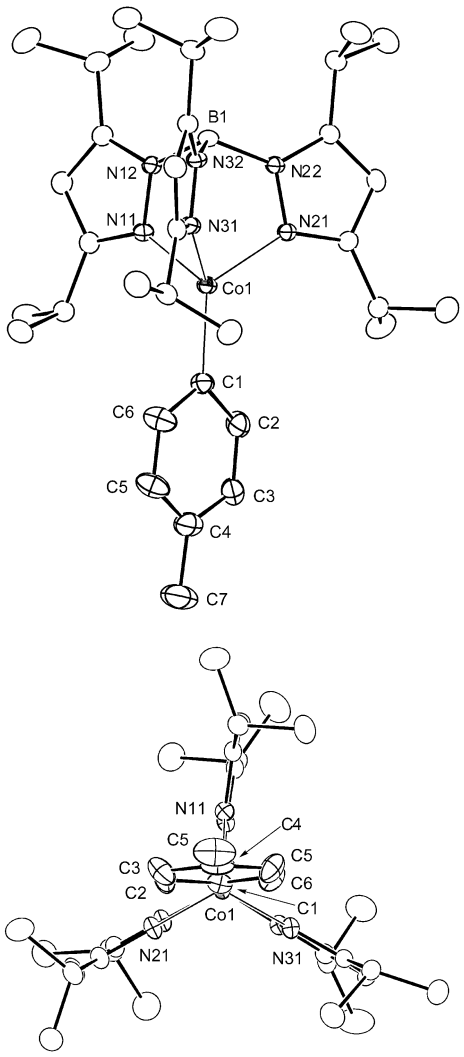

Figure 4. Molecular structure of **2** showing 30% thermal ellipsoids.

Scheme 6

Reactivity of **1** and **2**.

	$Tp^{iPr2}Co-C\equiv C-R$ **1**	$Tp^{iPr2}Co-C_6H_4-Me$ **2**
H^+	HC≡CR	H−C$_6$H$_4$−Me
O_2	no reaction	unidentified product
RC≡CH	linear trimerization (R=CO_2Me; **1a**)	$Tp^{iPr2}Co-C\equiv C-R$ (**1**)
$RHC=CH_2$	no reaction	
CO	no reaction	$Tp^{iPr2}Co(CO)-C_6H_4-Me$

(i) Stability. Both of the complexes were readily hydrolyzed by moisture to give the corresponding hydrocarbons and the hydroxo complex **4**. The protonation of the Co−C bond in **1** supports the weak back-donation discussed above, because effective back-donation usually induces reaction with electrophiles at the β-carbon atom (Scheme 7).[21] The *p*-tolyl complex **2** decomposed upon exposure to O_2 atmosphere in a manner similar to the

(23) The experimental result that the bent structure is more stable than the linear structure could not be reproduced by the EHMO calculation. The linear structure (**B**) is calculated to be more stable than the bent structure (**B**-bent) by ca. 6 kcal/mol. But because the difference is too small when the reliability of the EHMO calculation is taken into account, a more detailed calculation is needed to obtain a definitive conclusion. But the present consideration provides a qualitative explanation.

(24) An analytically pure sample of **2** could not be obtained despite many attempts due to contamination of a small amount of $Tp^{iPr2}Co-Br$ as revealed by ^1H NMR.

(25) Silverstein, R. M.; Bassler, G. C.; Morrill, T. C. *Spectroscopic Identification of Organic Compounds*, 5th ed.; John Wiley & Sons: New York, 1991.

Scheme 7

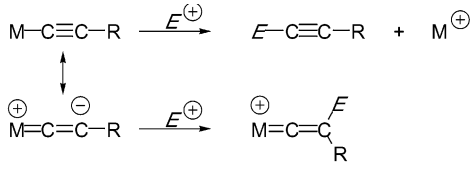

Scheme 8

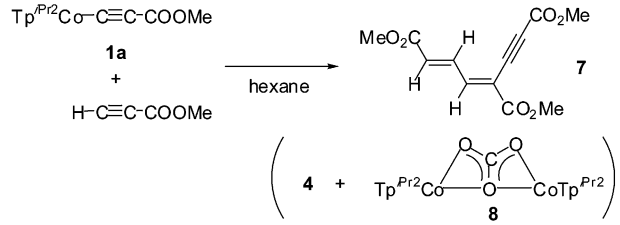

alkyl complexes, but the decomposition product could not be identified. The alkynyl complexes **1** were left unaffected by O_2-exposure. In addition, no significant thermal deterioration was observed for **1** and **2** by heating to 100 °C under inert atmosphere.

(ii) Reaction with Unsaturated Hydrocarbons Including Catalytic Linear Trimerization of Methyl Propiolate by 1a. We also examined reaction of **1a**,**c**,**d**,**e** and **2** with unsaturated hydrocarbons [1-alkynes (R−C≡C−H; R = Ph, *n*-C_4H_9, COOMe), Ph−C≡C−Ph, 1-alkene (R−CH═CH_2; R = Ph, *n*-C_4H_9, COOMe)], but characterizable products were obtained only in the cases of the reaction of **1a** with H−C≡C−COOMe and carbonylation of **2** described below.[26] The sluggish reactivity of **1** and **2** could be attributed to the lack of a vacant coordination site (see above), as already discussed for the alkyl complexes.

When a benzene solution of **1a** and methyl propiolate was refluxed, catalytic linear trimerization proceeded to give the (*E*,*E*)-buta-1,3-dien-5-yne derivative **7** (Scheme 8). The reaction was slow, and, after heating for 20 h, ca. 14 equiv of methyl propiolate was converted to **7** (ca. 4.5 turnovers). The catalytic reaction was so specific that neither another stereoisomer nor oligomer was detected at all. The stereochemistry of the diene moiety was determined on the basis of the AMX ^{1}H NMR coupling pattern of the three adjacent olefinic protons on the diene linkage and the strong IR absorption at 983 cm^{-1},[25] and the configuration of the C(H)−C≡C−COOMe moiety is assigned on the assumption of *cis*-stereochemistry of the insertion process (see below). ^{13}C NMR and GC−MS data consistent with the structure were also obtained (see Experimental Section). The reaction proceeded as long as the blue color of the reaction mixture was retained, and color change to green was an indication of deactivation of the catalytic species. ^{1}H NMR analysis of the green reaction mixture revealed formation of the dinuclear μ-carbonato complex **8**,[27] which should be formed by interaction of the hydroxo complex **4** (formed via hydrolysis of **1a**) with adventitious CO_2. The catalytic species **1a** could be regenerated via interaction of the hydroxo complex **4** with methyl propiolate present in the mixture but could not be formed from the μ-carbonato complex **8**.

A plausible formation mechanism of **7** should involve double coordination−insertion of the C≡C bond in methyl propiolate into the Co−C≡ bond in **1a**: **1a** → Tp^{iPr2}Co−CH═C(E)−C≡C−E **F** → Tp^{iPr2}Co−CE═CH−CH═C(E)-C≡C−E **G** (E = COOMe). Hydrolysis of the Co−C═ bond in **G** with a third equivalent of methyl propiolate would furnish the linear trimer **7**. The final intermediate **G** could be detected by a deuteration experiment. When a reaction mixture was quenched by CH_3COOD at an early stage of the catalytic reaction (3 h), ca. 40% of **7**-d_1 was detected by GC−MS analysis, and analysis after 23 h revealed less than 5% deuteration. The decrease of the extent of deuteration after a prolonged reaction time is due to catalytic formation of **7** as well as deterioration of the catalytic species discussed above, i.e., irreversible conversion to **8**. Notable points of this mechanism are (1) the different orientation of the alkyne substrate in the two insertion steps and (2) the specific formation of the linear trimer **7** as a sole organic product. As for point (1), although the second insertion giving **G** may be explained in terms of a Michael addition-type mechanism, we have no explanation for the regiochemistry of the first insertion giving **F**. A radical mechanism may be viable, as suggested by one of the reviewers, because homolysis of the M−C bond in $Tp^{R'}$M−alkyl-type complexes has been noted.[3,4] But we have no experimental evidence that supports any mechanism (except for **G**, see above). Point (2) could be interpreted in terms of the steric environment around the Co−C bond. The α-carbon atoms of the intermediates **F** and **G** carry the H and COOMe group, respectively. Because the Co−C bond in the latter intermediate **G** is sterically congested due to the ester group at the α-carbon atom, interaction with another molecule of methyl propiolate leading to oligomerization should be hindered, and, instead, protonolysis of the polar Co−C bond with the acidic terminal hydrogen atom of methyl propiolate leads to the formation of **7**, accompanying regeneration of the catalytic species **1a**. The stereochemistry of **7** should be determined by the *cis*-stereochemistry of the insertion steps. Although catalytic oligomerizations of alkynes such as linear oligomerization giving oligoenyne compounds and cyclic oligomerization of alkynes giving, for example, benzene and cyclooctatriene derivatives have many precedents,[28] to our knowledge only two examples of

(26) Reaction of **1h** and Ph−C≡C−H gave an unidentified product. Reaction of **1d** with Me_3Si−C≡C−H in refluxing benzene gave the siloxo complex, Tp^{iPr2}Co−OSiMe_3, which was also characterized by X-ray crystallographic (Figure S4)[14] and spectroscopic methods. [Data for Tp^{iPr2}Co−OSiMe_3: ^{1}H NMR (C_6D_6): δ_H 73.8 (3H, 4-pz-H), 12.4 (3H, C*H*Me_2), 3.1 (9H, SiMe_3), 2.8 (3H, C*H*Me_2), 1.8, 1.5 (18H × 2, CH*Me*$_2$), −21.5 (1H, BH). IR: ν_{BH} 2543 cm^{-1}. UV−vis: λ_{max}/nm (ϵ/M^{-1}·cm^{-1}) 820 (21), 654 (630), 582 (233), 295 (300). Anal. Calcd for $C_{30}H_{55}N_6$OBSiCo: C, 58.72; H, 9.03; N, 13.70. Found: C, 58.35; H, 9.05; N, 13.51.] Tp^{iPr2}Co−OSiMe_3 should be formed from **4** (formed by hydrolysis of **1d**) and Me_3Si−C≡C−H following the mechanism shown in Scheme 3 (path *b*). Although such a reaction does not occur at ambient temperature (under the conditions for Scheme 2), reaction under forced conditions for a prolonged period may form the thermodynamically more stable siloxo complex.

(27) For $Tp^{R'}$M(κ^2-carboxylato) complexes, see, for example: Ogihara, T.; Hikichi, S.; Akita, M.; Uchida, T.; Kitagawa, T.; Moro-oka, Y. *Inorg. Chim. Acta* **2000**, *297*, 162.

(28) Cornils, B.; Herrmann, W. A. *Applied Homogeneous Catalysis with Organometallic Compounds*; VCH: Weinheim, 1996. Ohmura, T.; Yamamoto, Y.; Miyaura, N. *J. Am. Chem. Soc.* **2000**, *122*, 4990−4991. Ohmura, T.; Yorozuya, S; Yamamoto, Y.; Miyaura, N. *Organometallics*

Scheme 9

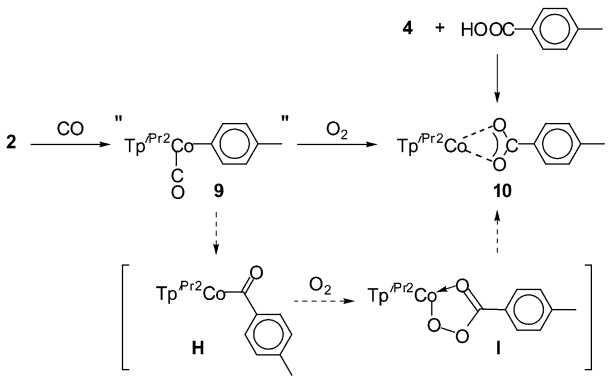

linear trimerization appeared, as reported by Klein[29] and Furlani.[30]

(iii) Carbonylation. The *p*-tolyl complex **2** was readily carbonylated upon exposure to CO (1 atm) to give a brown mixture (Scheme 9), while the alkynyl complexes **1** remained unreacted even under pressurized conditions (5 atm). A ^{1}H NMR spectrum of the brown reaction mixture containing a broad signal at δ 1.9[31] is distinct from that of **2**, suggesting formation of a new species with a different coordination geometry. Because (1) the IR spectrum of the reaction mixture contained an intense ν_{CO} vibration (2013 cm^{-1}) in addition to the ν_{BH} absorption (2535 cm^{-1})[15] and (2) no $\nu_{C=O}$ vibration of an acyl-metal functional group was detected, the product **9** was assigned to the CO-coordinated species. Despite many attempts **9** could not be isolated, and purple crystals of **10** that crystallized out of the solution were characterized by X-ray crystallography (Figure S4)[32] to be the κ^2-carboxylato complex **10**, which was confirmed by comparison with an authentic sample obtained by dehydrative condensation between **4** and *p*-toluic acid. Exposure of a brown mixture containing **9** to O_2 caused an immediate color change to blue (**10**). A plausible formation mechanism of **10** shown in Scheme 9 involves successive CO and O_2 insertion into the Co−C bond in **9** to give the acyl (**H**) and acylperoxo intermediates (**I**), and decomposition of **I** should produce the carboxylato complex **10**. An acylperoxometal species has been regarded as a key intermediate of metal-catalyzed oxidation of organic compounds,[33] and its reactivity as an oxidant is now under further study. The result of carbonylation of the *p*-tolyl complex **2** is in contrast to that of the alkyl complex, Tp$^{i\mathrm{Pr}2}$Co−R, which afforded the carbonyl-acyl species Tp$^{i\mathrm{Pr}2}$Co(CO)−C(=O)−R. The difference could be ascribed to the nucleophilicity of the hydrocarbyl groups: alkyl groups coordinated at the C(sp^3) atom versus aryl groups coordinated at the C(sp^2) atom, the former with more p-character being more nucleophilic.[34]

Conclusions. A series of Tp$^{R'}$Co−R-type hydrocarbyl complexes containing Co−C(sp^n) bonds (n = 1−3) are prepared and characterized successfully, when the previous results on the alkyl complexes[3] are combined with the present results. Despite their highly electron-deficient electronic structures, the hydrocarbyl complexes turn out to be thermally stable species. It is notable that β-hydride elimination (for alkyl complexes) and oligomerization (for alkynyl and aryl complexes; Scheme 1), which are viable decomposition processes for normal hydrocarbyl complexes, do not operate for the Tp$^{R'}$Co−R complexes. Such an unusual behavior should be a result of the lack of vacant frontier orbitals, which originates from the property of the Tp$^{R'}$ ligand as a tetrahedral enforcer. Tetrahedral structures with frontier orbitals of a small energy separation (Figure 5: **J**45−49, **K**56−60, **L**46−50) cause high-spin electronic configurations,[22] where all frontier orbitals accommodate an electron pair or an unpaired electron.

σ-Bonding interaction is the dominant character of the metal−carbon bonding interaction in the Tp$^{R'}$Co−R complexes (Figure 5). Because, however, (1) no additional orbital mixing occurs due to only one of each σ-type orbital being included in the TpCo and R fragments (**C**43−**M**4/**N**15/**O**5) and (2) the energy separation between the two σ-type orbital is substantial, the covalent character of the Co−C bond is not significant and, as a result, the Co−C bond is so polarized as to be readily protonated even by moisture in the air. On the other hand, π-bonding interaction is virtually negligible for the alkynyl (**L**) and aryl complexes (**K**). A small contribution of back-donation is observed, only when an electron-withdrawing substituent such as C(=O)−X groups is attached to the π-system.

Despite the 15-electron configuration of the Tp$^{R'}$Co−R complexes, which is short of the coordinatively saturated 18-electron configuration, they turn out to be sluggish toward organic substrates, in particular, unsaturated hydrocarbons, and the sluggishness could be ascribed again to the lack of vacant frontier orbitals as mentioned above. However, as typically exemplified by the regio- and stereospecific linear trimerization of methyl propiolate catalyzed by **1a**, interaction of the Tp$^{R'}$Co−R species with an organic compound may induce perturbation of their electronic structure to provide an opportunity to exhibit unprecedented reactivity.

Experimental Section

General Procedures. All manipulations were carried out under an Ar atmosphere using standard Schlenk tube techniques. THF, ether, toluene, pentane, and hexane were dried over Na−K/benzophenone under Ar and distilled just before use. ^{1}H NMR spectra were recorded on a Bruker AC200 spectrometer (^{1}H: 200 MHz). Benzene-d_6 and toluene-d_8 for NMR measurements containing 0.5% TMS were dried over molecular sieves and distilled under reduced pressure. IR and UV spectra were obtained on JASCO FT/IR 5300 and V-570 spectrometers, respectively. FD-MS spectra were obtained on a JEOL JMS-700 mass spectrometer. Magnetic susceptibility was measured on a Sherwood Scientific MSB-AUTO. Organic products were identified and quantified by a combination of

1999, *18*, 365−367. Miyaura, N.; Suzuki, A. *Chem. Rev.* **1995**, *95*, 2457. Yi, C. S.; Liu, N. *Organometallics* **1998**, *17*, 3158−3160. Pavlic, S.; Gemel, C.; Slugovc, C.; Mereiter, K.; Schmid, R.; Kirchner, K. *J. Organomet. Chem.* **2001**, *617*−*618*, 301. See also references cited in these papers.

(29) Klein, H. F.; Marger, M. *Organometallics* **1992**, *11*, 3174.

(30) Carusi, P.; Cerichelli, G.; Furlani, A.; Russo, M. V.; Suber, L. *Appl. Organomet. Chem.* **1987**, *1*, 555

(31) Other signals could not be located presumably due to broadening, but complete conversion of **2** could be verified by the ^{1}H NMR analysis.

(32) Kitajima, N.; Hikichi, S.; Moro-oka, Y. *J. Am. Chem. Soc.* **1993**, *115*, 5496.

(33) Ohzu, Y.; Hikichi, S.; Akita, M. Unpublished result.

(34) Berke, H.; Hoffmann, R. *J. Am. Chem. Soc.* **1978**, *100*, 7224.

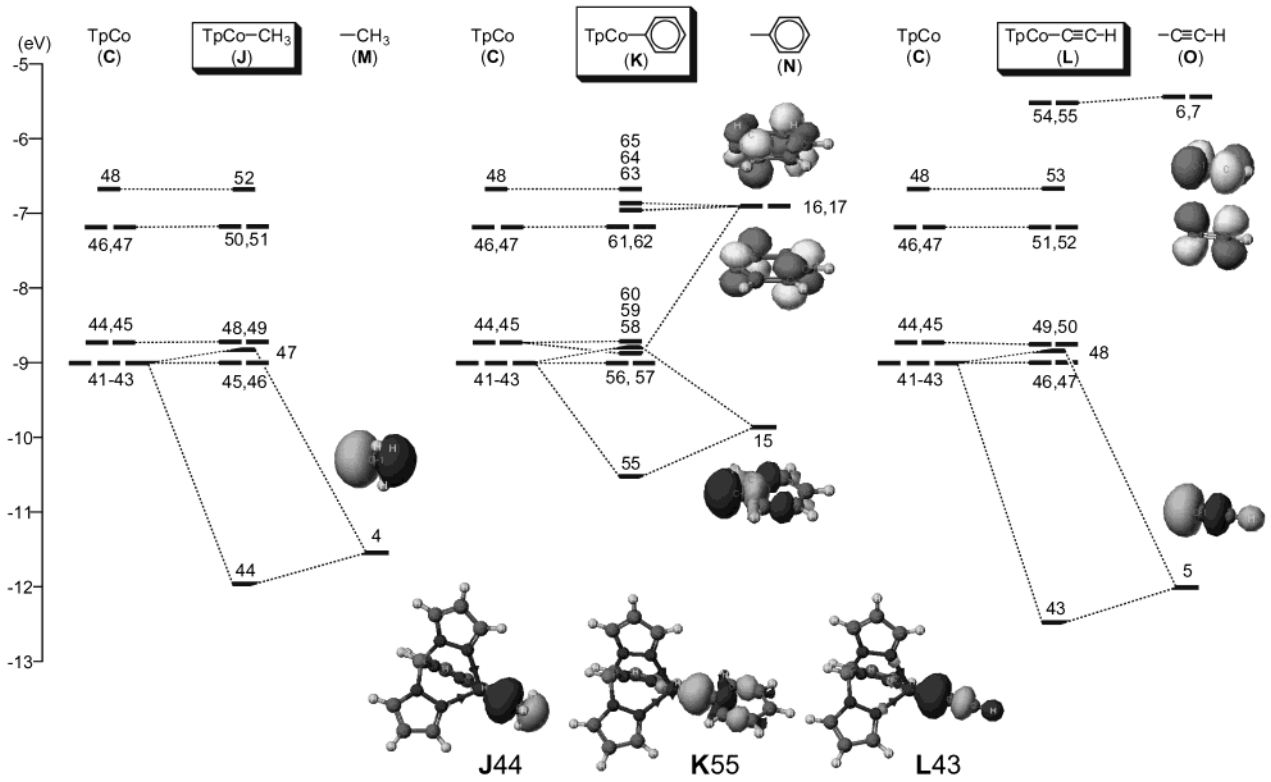

Figure 5. Comparison of molecular orbitals of TpCo−Me (**J**), −Ph (**K**), and −C≡C−H (**L**).

GLC (Shimadzu GC17A equipped with a PHA0201 capillary column and an FID detector) and GC−MS analyses (Shimadzu QP5000 connected to GC17A equipped with a PHA0201 capillary column). EHMO calculations were done using the CAChe system (ver. 4.0). The chloro (**3**, **3′**) and hydroxo complexes (**4**, **4′**) were prepared according to literature procedures.[32] Other chemicals were used as received without further purification.

Preparation of Alkynyl Complexes (1). As a typical example, the synthetic procedure for **1a** is described below in detail, and the other derivatives were prepared in essentially the same method unless otherwise stated. Yield, reaction time, and spectroscopic data for **1** are shown in Scheme 2 and Table 1.

Tp^{iPr2}Co−C≡C−COOMe (1a). To a 50 mL Schlenk tube containing a hexane solution (25 mL) of **3** (181 mg, 0.167 mmol) and molecular sieves (ca. 1.0 g) was added methyl propiolate (34 mg, 0.401 mmol) via a microsyringe. The color of the solution changed from red (the color of **3**) to blue upon mixing, and the resultant mixture was stirred for 3 h. Then the molecular sieves were removed by filtration and removal of the volatiles under reduced pressure gave blue powers, crystallization of which from hexane at −30 °C gave **1a** (152 mg, 0.250 mmol, 75% yield) as blue crystals. **1a**: $\mu_{eff} = 3.4\ \mu_B$. λ_{max}/nm (ϵ/M^{-1}·cm^{-1}; in hexane): 290 (1521), 646 (888), 888-(121). FD-MS: *m*/*z* 607 (M$^+$). Anal. Calcd for $C_{31}H_{49}N_6O_2BCo$: C, 61.29; H, 8.13; N, 13.83. Found: C, 61.02; H, 8.30; N, 13.76. **1b**: $\mu_{eff} = 3.4\ \mu_B$. λ_{max}/nm (ϵ/M^{-1}·cm^{-1}; in hexane): 290 (1177), 646 (815), 860 (130), 886 (115). FD-MS: *m*/*z* 607 (M$^+$). Anal. Calcd for $C_{31}H_{51}N_6O_2BCo$: C, 61.84; H, 8.27; N, 13.52. Found: C, 61.53; H, 8.34; N, 13.23. **1c**: $\mu_{eff} = 3.6\ \mu_B$. λ_{max}/nm (ϵ/M^{-1}·cm^{-1}; in hexane): 290 (1653), 300 (1639), 646 (1080), 866 (128), 892 (153). FD-MS: *m*/*z* 591 (M$^+$). Anal. Calcd for $C_{31}H_{49}N_6$-OBCo: C, 62.95; H, 8.35; N, 14.21. Found: C, 62.51; H, 8.40; N, 13.93. **1d**: $\mu_{eff} = 3.6\ \mu_B$. λ_{max}/nm (ϵ/M^{-1}·cm^{-1}; in hexane): 299 (1019), 313 (1004), 657 (776). FD-MS: *m*/*z* 621 (M$^+$). Anal. Calcd for $C_{32}H_{55}N_6BSiCo$: C, 61.83; H, 8.92; N, 13.52. Found: C, 61.93; H, 8.99; N, 12.82. **1e**: $\mu_{eff} = 3.5\ \mu_B$. λ_{max}/nm (ϵ/M^{-1}·cm^{-1}; in hexane): 297 (820), 313 (918), 658 (800), 887 (73). FD-MS: *m*/*z* 663 (M$^+$). Anal. Calcd for $C_{35}H_{61}N_6BSiCo$: C, 63.34; H, 9.26; N, 12.66. Found: C, 63.36; H, 9.58; N, 12.41. **1g**: λ_{max}/nm (ϵ/M^{-1}·cm^{-1}; in hexane): 297 (1154), 654 (678), 889 (96), 906 (98). FD-MS: *m*/*z* 549 (M$^+$). **1h**: λ_{max}/nm (ϵ/M^{-1}·cm^{-1}; in hexane): 310 (2554), 663 (685). FD-MS: *m*/*z* 625 (M$^+$). **1i**: λ_{max}/nm (ϵ/M^{-1}·cm^{-1}; in hexane): 306 (735), 318 (735), 662 (449), 888 (35). Analytically pure samples of **1g**−**i** could not be obtained as described in the main text.

Reaction of 3 with Ph$_3$Si−C≡C−H: Formation of Tp^{iPr2}Co−OSiPh$_3$ (5). Reaction of **3** (238 mg, 0.220 mmol) with Ph$_3$Si−C≡C−H (188 mg, 0.660 mg) as described for the synthesis of **1a** gave **5** (235 mg, 0.294 mmol, 68% yield) as blue needles. **5**: ^{1}H NMR (C_6D_6): δ_H 74.9 (3H, 4-pz-H), 9.7 (6H, Ph), 7.9 (6H, Ph), 7.4 (3H, Ph), 3.2 (18H, CH*Me$_2$*), 2.7 (3H, C*H*Me$_2$), 1.7 (18H, CH*Me$_2$*). IR: ν_{BH} 2544 cm^{-1}. UV−vis: λ_{max} (ϵ/M^{-1}·cm^{-1}) 438 (465), 508 (39), 791 (75), 916 (120). Anal. Calcd for $C_{45}H_{31}N_6OBSiCo$: C, 67.57; H, 7.69; N, 10.51. Found: C, 67.42; H, 7.46; N, 10.32. The nickel derivative **5′** was prepared in essentially the same method. **5′** (70% yield, red crystals): ^{1}H NMR (C_6D_6): δ_H 79.2 (3H, 4-pz-H), 8.3 (6H, Ph), 8.0 (6H, Ph), 7.8 (3H, Ph), 3.1 (18H, CH*Me$_2$*), 1.4 (18H, CH*Me$_2$*), 0.85 (3H, C*H*Me$_2$). IR: ν_{BH} 2538 cm^{-1}. UV−vis: λ_{max} (ϵ/M^{-1}·cm^{-1}) 438 (465), 508 (39), 791 (75), 916 (120). Anal. Calcd for $C_{45}H_{31}N_6OBSiNi$: C, 67.60; H, 7.69; N, 10.51. Found: C, 67.68; H, 7.74; N, 10.29.

Synthesis of Tp^{iPr2}Co-*p*-tol (2). To an ethereal solution (10 mL) of **4** (136 mg, 0.243 mmol) cooled at −78 °C was added *p*-tol-MgBr (0.65 M ethereal solution, 0.37 mL, 0.32 mmol), and the resultant mixture was gradually warmed to room temperature. The color of the mixture changed from blue to green. When the temperature reached room temperature, the volatiles were removed under reduced pressure and the products were extracted with pentane and filtered through a glass filter. Concentration and cooling to −30 °C gave **2** (117 mg, 0.190 mmol, 78% yield) as blue crystals.[24] **2**: UV−vis: λ_{max} (ϵ/M^{-1}·cm^{-1}) 586 (326), 621 (438), 669 (sh, 891), 697 (1304), 951 (46).

Linear Trimerization of Methyl Propiolate Catalyzed by 1a: Formation of 7. A benzene solution (10 mL) containing **1a** (32.8 mg, 0.054 mmol) and methyl propiolate (136 mg, 1.62 mmol) was refluxed for 14 h. Removal of the volatiles

Table 3. Crystallographic Data

	1a	**1e**	**2**	**5**
formula	$C_{31}H_{49}BN_6O_2Co$	$C_{35}H_{61}BN_6Si'Co$	$C_{34}H_{53}BN_6Co$	$C_{45}H_{61}BN_6OSiCo$
fw	607.50	663.73	615.56	799.83
cryst syst	orthorhombic	monoclinic	monoclinic	monoclinic
space group	$P2_12_12_1$	$P2_1$	$P2_1/n$	$P2_1/c$
a/Å	17.9286(7)	14.1440(4)	9.3235(4)	9.476(2)
b/Å	21.6998(8)	31.3152(8)	15.3962(7)	24.278(3)
c/Å	8.7517(2)	9.5739(2)	24.3715(8)	19.695(4)
β/deg		108.074(1)	93.506(4)	95.902(4)
V/Å^3	3404.8(2)	4031.3(2)	3853.9(6)	4507(2)
Z	4	4	4	4
d_{calcd}/g·cm^{-3}	1.185	1.094	1.177	1.179
μ/mm^{-1}	0.539	0.485	0.525	0.447
oscillation range/deg	180 (3° step)	180 (2° step)	180 (5° step)	180 (4° step)
no. of oscillation images	60	90	36	45
exposed time/s·deg^{-1}	400	950	360	840
no. of variables	383	823	392	496
R1 for data	0.049	0.052	0.052	0.130
with $I > 2\sigma(I)$	(for 3722 data)	(for 5869 data)	(for 4647 data)	(for 2918 data)
wR2	0.129	0.144	0.145	0.312
	(for all 4341 data)	(for all 8957 data)	(for all 7514 data)	(for all 9117 data)

	5′·hexane$_{1/2}$	**10**	Tp^{iPr2}Co−OSiMe$_3$
formula	$C_{48}H_{68}BN_6OSiNi$	$C_{35}H_{53}BN_6O_2Co$	$C_{30}H_{55}BN_6OSiCo$
fw	842.69	659.57	613.63
cryst syst	monoclinic	monoclinic	monoclinic
space group	$P2_1/n$	$P2_1/n$	$C2/c$
a/Å	19.377(1)	9.449(1)	35.122(2)
b/Å	13.749(1)	15.7388(9)	9.5247(3)
c/Å	20.130(1)	25.962(1)	24.002(1)
β/deg	116.475(2)	96.615(2)	115.634(1)
V/Å^3	4800.7(5)	3475.2(2)	7238.8(5)
Z	4	4	8
d_{calcd}/g·cm^{-3}	1.166	1.137	1.126
μ/mm^{-1}	0.469	0.481	0.537
oscillation range/deg	180 (5° step)	180 (5° step)	180 (5° step)
no. of oscillation images	36	36	36
exposed time/s	420	1200	720
no. of variables	524	414	376
R1 for data	0.068	0.125	0.063
with $I > 2\sigma(I)$	(for 5689 data)	(for 1591 data)	(for 5753 data)
wR2	0.195	0.309	0.172
	(for all 10 740 data)	(for all 8197 data)	(for all 8129 data)

under reduced pressure left a brown solid, washing of which with hexane several times gave **7** as a pale brown solid (16 mg, 337%). **7**: ^{1}H NMR (C_6D_6): δ_H 7.76 (1H, dd, J = 11.9 and 15.2 Hz, $MeO_2CCH{=}CH{-}CH{=}$), 7.42 (1H, dd, 0.8 and 11.9 Hz, $MeO_2CCH{=}CH{-}CH{=}$), 5.79 (1H, dd, J = 0.8 and 15.2 Hz, $MeO_2CCH{=}CH{-}CH{=}$), 3.284, 3.276, 3.17 (3H × 3, s × 3, OMe). ^{13}C NMR (C_6D_6): δ_C 165.3, 163.3 (=C-*C*OOMe), 153.5 (≡C−*C*OOMe), 148.0, 137.5, 131.9, 118.9 (s × 4, C=C), 90.7 (*C*≡C−COOMe), 78.7 (C≡*C*−COOMe), 52.5, 52.3, 51.5 (OMe). IR: $\nu_{=CH}$ 3080, $\nu_{C\equiv C}$ 2212, $\nu_{C=O}$ 1718, $\nu_{C=C}$ 1631, δ_{CH} 983 cm^{-1}. GC−MS: m/z 252 (M^+). Anal. Calcd for $C_{12}H_{12}O_6$: C, 57.14; H, 4.80. Found: C, 57.57; H, 4.93.

Carbonylation−Oxygenation of 3: Formation of 10. Exposure of a pentane solution (10 mL) of **3** (117 mg, 0.189 mmol) to CO (from a rubber balloon) caused a color change from blue to brown. Evacuation for a short period followed by filling with O_2 gas gave a blue solution, from which **10** (51 mg, 0.078 mmol, 41% yield) was isolated as purple crystals after concentration and cooling at −30 °C. **10**: ^{1}H NMR (C_6D_6) δ_H 64.4 (3H, 4-pz), 58.9 (1H, BH), 52.2 (2H, *p*-tol), 37.2 (3H, Me in *p*-tol), 24.6 (2H, *p*-tol), 16.9 (3H, C*H*Me$_2$), 13.1 (18H, CH*Me*$_2$), −24.6 (18H, CH*Me*$_2$), −61.7 (3H, C*H*Me$_2$). IR: ν_{BH} 2529, $\nu_{C=C}$(Ar) 1685 cm^{-1}. Anal. Calcd for $C_{35}H_{53}N_6O_2BCo$: C, 63.73; H, 8.10; N, 12.74. Found: C, 63.46; H, 8.30; N, 12.24. An authentic sample of **10** was prepared by the reaction of **3** with *p*-toluic acid. Addition of (55.3 mg, 0.406 mmol) to an ethereal solution (10 mL) of **3** (200 mg, 0.185 mmol) caused an immediate color change from orange to purple. Removal of the volatiles under reduced pressure followed by crystallization from acetonitrile at −30 °C gave **11** (141 mg, 0.215 mmol, 58% yield).

X-ray Crystallography. Crystallographic data are summarized in Table 3. Single crystals of **1a**, **1e**, **5**, **5′**, **10**, Tp^{iPr2}-Co−OSiMe$_3$ (hexane), and **2** (pentane) were obtained by recrystallization from the solvents shown in the parentheses and mounted on glass fibers. Details for **5**, **5′**, **10**, and Tp^{iPr2}-Co−OSiMe$_3$ are included in the Supporting Information.

Diffraction measurements were made on a Rigaku RAXIS IV imaging plate area detector with Mo Kα radiation (λ = 0.71069 Å) at −60 °C. Indexing was performed from two oscillation images, which were exposed for 5 min. The crystal-to-detector distance was 110 mm ($2\theta_{max}$ = 55°). Readout was performed with the pixel size of 100 μm × 100 μm. Neutral scattering factors were obtained from the standard source. In the reduction of data, Lorentz and polarization corrections and empirical absorption corrections were made.[35] Crystallographic data and results of structure refinements are listed in Table 3.

The structural analysis was performed on an IRIS O2 computer using the teXsan structure solving program system obtained from the Rigaku Corp., Tokyo, Japan.[36] Neutral scattering factors were obtained from the standard source.[37]

The structures were solved by a combination of the direct methods (SHELXS-86[38] or SAPI91 or SIR92 or MITHRIL90)[39]

(35) Higashi, T. *Program for Absorption Correction*; Rigaku Corp.: Tokyo, Japan, 1995.

and Fourier synthesis (DIRDIF94).[40] Least-squares refinements were carried out using SHELXL-97[38] (refined on F^2) linked to teXsan. All the non-hydrogen atoms were refined anisotropically. Unless otherwise stated, riding refinements were applied to the methyl hydrogen atoms [B(H) = B(C)], and the other hydrogen atoms were fixed at the calculated positions. Details of the refinements were as follows. **5′**: The hexane solvate was refined isotropically and the disordered part was refined taking into account two components (C73: C73A = 0.5:0.5). Hydrogen atoms attached to it were not included in the refinement. **10**: The boron atom (B1) was refined isotropically.

Acknowledgment. We are grateful to the Ministry of Education, Culture, Sports, Science and Technology of the Japanese Government for financial support of this research (Grant-in-Aid for Scientific Research on Priority Areas: 11228201).

Supporting Information Available: Table of positional parameters and B_{eq}, anisotropic thermal parameters, and interatomic distances and bond angles. This material is available free of charge via the Internet at http://pubs.acs.org.

OM020268U

(36) *teXsan; Crystal Structure Analysis Package, ver. 1. 11*; Rigaku Corp.: Tokyo, Japan, 2000.

(37) *International Tables for X-ray Crystallography*; Kynoch Press: Birmingham, 1975; Vol. 4.

(38) (a) Sheldrick, G. M. *SHELXS-86: Program for crystal structure determination*; University of Göttingen: Göttingen, Germany, 1986. (b) Sheldrick, G. M. *SHELXL-97: Program for crystal structure refinement*; University of Göttingen: Göttingen, Germany, 1997.

(39) (a) SAPI91: Fan, H.-F. *Structure Analysis Programs with Intelligent Control*; Rigaku Corp.: Tokyo, Japan, 1991. (b) SIR92: Altomare, A.; Burla, M. C.; Camalli, M.; Cascarano, M.; Giacovazzo, C.; Guagliardi, A.; Polidori, G. *J. Appl. Crystallogr.* **1994**, *27*, 435. (c) MITHRIL90: Gilmore, C. J. *MITHRIL−an integrated direct methods computer program*; University of Glasgow: Glasgow, UK, 1990.

(40) Beurskens, P. T.; Admiraal, G.; Beurskens, G.; Bosman, W. P.; Garcia-Granda, S.; Gould, R. O.; Smits, J. M. M.; Smykalla, C. *The DIRDIF program system;* Technical Report of the Crystallography Laboratory; University of Nijmegen: Nijmegen, The Netherlands, 1992.